

A possible activity cycle in Proxima Centauri

C. Cincunegui^{1,2,*}, R. F. Díaz^{1,2,*}, and P. J. D. Mauas^{1,3,*}

¹ Instituto de Astronomía y Física del Espacio, C.C. 67 Suc. 28 (1428) Buenos Aires, Argentina

² Fellow of the CONICET

³ Member of the Carrera del Investigador Científico, CONICET

Received [date]; accepted [date]

ABSTRACT

Context. Several late-type stars present activity cycles resembling the Solar one. This fact has been observed mostly in stars ranging from F to K, i.e., in stars with a radiative core and an outer convective layer.

Aims. This work aims at studying whether an activity cycle can be detected in the dM5.5e star Proxima Centauri, which is supposed to be completely convective.

Methods. We present periodical medium-resolution echelle observations covering the complete visual range, which were taken at the CASLEO Argentinean Observatory. These observations are distributed over 7 years. We discarded the spectra that present flare activity, and analyze the remaining activity levels using four different statistical techniques to look for a period of activity.

Results. We find strong evidence of a cyclic activity, with a period of ~ 442 days. We also estimate that the Ca II *S* index varies around 130% due to activity variations outside of flares.

Key words. Stars: activity – Stars: chromospheres – Stars: flare – Stars: individual: Proxima Centauri

1. Introduction

It is generally accepted that magnetic activity in late-type stars, and in particular activity cycles like the one observed in the Sun, are the product of the $\alpha\Omega$ dynamo, which results from the action of differential rotation at the tachocline (the interface between the convective envelope and the radiative core). Therefore, the presence and characteristics of activity cycles are closely related to the existence and depth of an outer convection zone. Since this depth depends on spectral type – from F stars that have shallow convection zones to middle M stars that are totally convective –, it is of special interest to study these cycles in stars of different spectral types, and in particular in middle-M stars, to determine whether there is an onset of cyclic activity.

To date, activity cycles have been detected in several late-type stars (see, for example, Baliunas et al. 1985), mainly measuring variations in the well known *S* index, essentially the ratio of the flux in the core of the Ca II H and K lines to the continuum nearby. This index has been defined at the Mount Wilson Observatory, where an extensive database of activity has been built over the last three decades. However, these observations are mainly concentrated on stars ranging from F to K (see, for example, Baliunas et al. 1995), due to the long exposure times needed to observe the Ca II lines in the red and faint M stars. As a contribution to the subject, we explore the existence of an activity cycle in the dM5.5e star Proxima Centauri, using observations we made at the CASLEO Observatory, in Argentina and that span 7 years.

The triple star system α Cen is located at 1.3 pc from the Sun. One of its members is Proxima Centauri (α Cen C; GJ551), the closest star to Earth, which has a visual magnitude of 11.01. Prox Cen has an effective temperature of 3042 K (Ségransan et al. 2003), a radius of $\sim 1/7 R_{\odot}$ (Pettersen 1980), and a mass of $\sim 0.2 M_{\odot}$ (Allen 1976). Its rotation period has been estimated several times. From photometric observations, Benedict et al. (1998a) found $P_{\text{rot}}=83.5$ days, while Doyle (1987) measured $P_{\text{rot}}=51 \pm 12$ days from chromospheric activity and Guinan & Morgan (1996), using IUE observations of *h* and *k* Mg II lines, found $P_{\text{rot}}=31.5 \pm 1.5$ days. These rotation periods are longer than in others M stars (see, for example, Barnes 2003). This longer period is consistent with the older age of Prox Cen. If Proxima is coeval with its two companions, its age should be 4-4.5 10^9 years (Demarque et al. 1986).

Prox Cen is also a very active star: it is the first star where evidence of a stellar corona outside flares was found (Haisch & Linsky 1980). Several flares have been observed in this star, not only in X rays (Reale et al. 1988, 2004; Güdel et al. 2002, 2004), but also in UV (Haisch et al. 1977), and simultaneously in both (Byrne & McKay 1989; Haisch et al. 1990). Some photometric and spectroscopic flares have been detected (Walker 1981; Patten 1994; Benedict et al. 1998b) and Slee et al. (2003) detected flares in radio waves.

Haisch et al. (1990) suggested that Proxima presents an activity cycle. Using UV observations, Guinan & Morgan (1996) observed that short-term activity variations have a minimum around 1995, and deduced from this fact that the activity cycle had a minimum at that year, although during that time four flares were detected. Benedict et al. (1998a) deduced the existence of an activity cycle with a period of about 1100 days from photometric observations.

This paper is organized as follows: In Sect. 2 we present our observations; in Sect. 3 we discuss possible activity indicators. We analyze whether our activity measurements are compatible

Send offprint requests to: C. Cincunegui, e-mail: carolina@iafe.uba.ar

* Visiting Astronomers, Complejo Astronómico El Leoncito, operated under agreement between the Consejo Nacional de Investigaciones Científicas y Técnicas de la República Argentina and the National Universities of La Plata, Córdoba and San Juan.

Table 1. Log of the observations. Column 1: a label used in the figures; Col. 2: $xJD=JD-2\,451\,000$, where JD is the Julian date; Col. 3: exposure time in minutes; Col. 4: spectrum clean of cosmic rays ('y') or not ('n') (whether it can be used in the Ca II and $H\alpha$ windows); spectra indicated with '-' do not include the corresponding region, those with '*' are the ones not used in Sect. 4, due to the presence of flares.

label	xJD	t	Ca/H α	label	xJD	t	Ca/H α	label	xJD	t	Ca/H α
0399a	241.85	25	-/y	0303a *	1 715.72	45	y/y	0904a	2 274.48	30	y/y
0399b	241.87	25	-/y	0303b	1 715.75	45	y/y	0904b	2 274.50	30	y/y
0399c	241.89	15	-/n	0303c	1 716.60	60	y/y	0305a	2 448.78	45	y/y
0399d	242.67	30	y/-	0303d	1 716.65	60	y/y	0305b *	2 448.81	45	y/y
0399e	242.70	30	y/-	0303e	1 716.69	60	y/y	0605a	2 523.55	60	y/y
0300a *	626.82	30	y/y	0303f	1 716.74	60	y/y	0605b	2 523.60	60	y/y
0300b *	626.84	30	y/y	0303g	1 716.78	60	y/y	0605c	2 523.64	60	y/y
0300c *	626.86	30	y/y	0303h	1 716.82	60	y/y	0605d	2 523.69	60	y/y
0300d *	626.88	30	y/y	0303i	1 716.87	60	y/y	0605e	2 523.74	60	y/y
0300e	627.82	45	y/y	0603a	1 804.59	45	n/n	0605f	2 523.78	60	y/y
0300f	627.86	45	y/y	0603b	1 804.63	45	n/n	0605g	2 543.60	90	n/y
0301a	972.78	60	y/y	0903a	1 895.51	33	y/y	0605h	2 543.66	90	n/y
0301b	972.83	60	y/y	0903b	1 895.53	33	y/y	0805a	2 600.51	80	y/y
0301c	974.70	90	y/y	0604a	2 160.59	45	n/y	0805b	2 600.57	80	y/y
0301d	974.77	90	y/y	0604b	2 160.63	45	n/y	0206a *	2 780.80	80	y/y
0701a	1 096.46	90	y/y	0604c	2 161.47	60	n/n	0206b	2 780.86	80	y/y
0701b	1 096.53	90	y/y	0604d	2 161.51	60	y/y	Total			49/53
0302	1 364.69	45	y/y	0604e	2 161.55	60	y/y				
0602a	1 451.66	45	y/y	0604f	2 161.61	60	y/y				
0602b	1 451.69	45	y/y	0604g	2 161.65	60	y/y				
0802a	1 519.50	45	y/y	0604h	2 161.69	60	y/y				
0802b *	1 519.53	45	y/y	0604i	2 161.73	60	n/n				

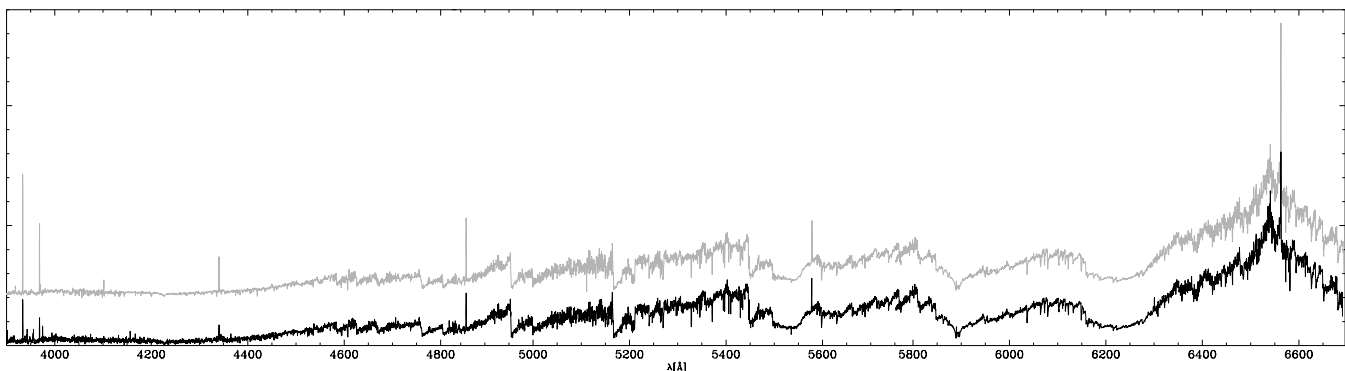


Fig. 1. In this figure we show two of the spectra with the best signal-to-noise relations for this star. Each of them is the combination of seven spectra with an exposure time of one hour. The upper spectrum was obtained in March 2003 (xJD 1716) and the one in the bottom in June 2004 (xJD 2161). They are arbitrarily displaced for clarity. It can be seen that the spectrum at the top shows a larger activity level.

with cyclic variations in Sect. 4. Finally, we summarize and discuss our results in Sect. 5.

2. The observations

Our observations were made at the 2.15 m telescope of the Complejo Astronómico El Leoncito (CASLEO), which is located at 2552 m above sea level, in the Argentinean Andes. We used a REOSC spectrograph to obtain medium-resolution echelle spectra covering the wavelength range 3900-7000 Å at a spectral resolution of $R=\lambda/\Delta\lambda \approx 26400$. We process the observations according to the method outlined in Cincunegui & Mauas (2004), obtaining flux-calibrated spectra. In Table 1 we show the observation log of Prox Cen. The first column includes

a label used in the figures, built from the month and year of the observation, and a letter to distinguish between different spectra from the same observation run; the second column lists $xJD=JD-2\,451\,000$, where JD is the Julian date at the beginning of the observation and the third column the exposure time (in minutes) of each observation. We inspected the regions of interest of each spectrum to determine if they were clean of cosmic rays: in the last column we indicated with 'y' or 'n' whether the spectra is suitable or not to be used in the windows corresponding to Ca II and $H\alpha$, as explained in the next section. With '-' we indicate some spectra that do not include the region of interest due to a different instrumental configuration.

There is a total of 60 individual observations, which have been carried out on 24 nights distributed over 7 years. In partic-

ular, on two of the nights we observed Proxima for seven hours, obtaining spectra with very high signal-to-noise ratios for this faint star, which are shown in Fig. 1. The upper spectrum corresponds to the observations on the night of March 17th, 2003 (spectra 0303c to 0303i), and the lower one was obtained the night of June 6th, 2004 (spectra 0604c to 0604i). Although no flares occurred on either night, as we will show, the overall activity level of the first one is much higher than that of the second one, as can be noted by the intensity of several chromospheric lines, in particular the Ca II and the Balmer lines, seen in emission in this dMe star.

3. Activity measurements

The widely-used S index from the Mount Wilson Observatory is the most common and best known chromospheric activity indicator for late-type stars. It is obtained from measurements taken with a four-channel spectrometer: two of the channels are centered in the cores of the H and K Ca II lines, with a triangular profile of 1.09 \AA FWHM, and the other two channels acquire the flux in the continuum nearby, in two passbands 20 \AA wide. The S index is built as the ratio between the chromospheric H and K fluxes and the photospheric continuum fluxes (Baliunas et al. 1998).

To reproduce Mount Wilson’s S index we integrated the fluxes in our spectra around the K and H Ca II lines, weighting them with a triangular profile resembling the instrumental response of the Mount Wilson spectrometer (Vaughan et al. 1978). We normalized these fluxes by the average flux in the same two

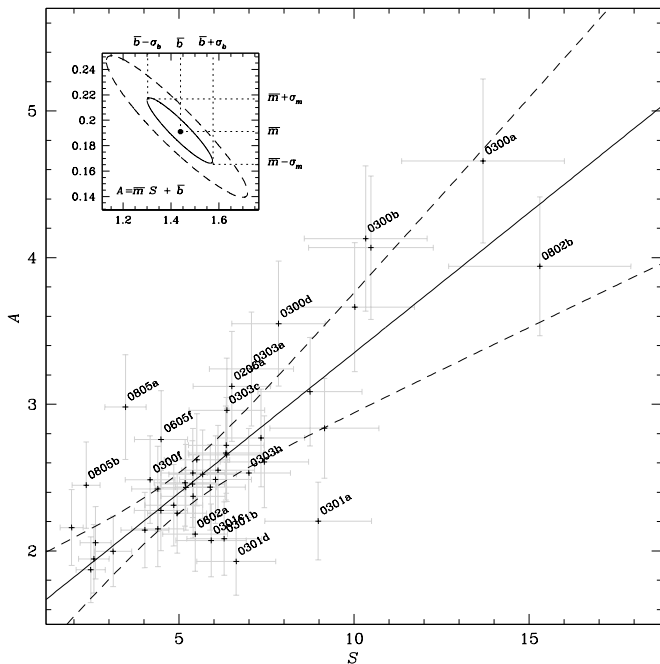


Fig. 2. Comparison of the Ca II index, S , and the $H\alpha$ index, A , for the 47 spectra in which both spectral features have been measured. The errors are assumed to be 12% in A and 17% in S . The least-squares fit has a slope of 0.19 ± 0.03 and a correlation coefficient of -0.94 . The fit significance is 60%. The dashed lines represent the points that deviate $\pm 3\sigma$ from the fit. In the small figure the confidence regions of 39.3% (full line) and 90% (dashed line) are drawn.

20 \AA continuum passbands used at Mount Wilson, centered at 3901 and 4001 \AA . In a previous work (Cincunegui & Mauas 2002), we checked the accuracy of our measurements observing a set of 18 non-variable stars given by Henry et al. (1996), and using them to intercalibrate our measurements with Mount Wilson’s S . We have found a very good correlation between both sets. However, Proxima Centauri is a very red and faint star ($B - V = 1.807$ and $V = 11.01$, Perryman et al. 1997). Therefore, the Ca II lines are very hard to observe with a good signal-to-noise ratio, requiring very long integration times with a 2m class telescope.

To overcome this problem, it is worth noting that in Proxima Centauri all the other Balmer lines, and in particular $H\alpha$, are observed in emission, as is the case for the most active late-type stars, the dKe and dMe stars. Therefore, we constructed an index A from the $H\alpha$ profile, defined as the ratio between the average flux in a 1.5 \AA square passband centered in the line and the average flux in a 20 \AA nearby continuum window, centered at 6605 \AA , in a similar way to the definition used for S .

To check whether A can be used as an activity index for this red star, we explored the relation between A and our S index, which is shown in Fig. 2. We estimated the errors in the flux-calibration method employed at 10% (Cincunegui & Mauas 2004). Therefore, 10% should be considered as a lower limit for the error in each index. Using a non-linear χ^2 minimization to fit a straight line considering the errors in both coordinates, and varying the percentual errors for each index until finding a reasonable significance of 60%, we found a very good correlation between both indexes, with a correlation coefficient of 0.94 and a slope of 0.19 for errors of 17% in S and 12% in A . The difference between the errors is natural since the Ca II lines have a much lower signal-to-noise ratio. In the insert to Fig. 2, we show the confidence regions for the parameters of the fit. In spite of the much lower sensitivity of $H\alpha$, as indicated by the small slope, we chose the A index to study activity in this star because of the much better signal-to-noise ratio.

Since Proxima is a flare star, it is expected to have frequent flares. Therefore, before exploring the existence of an activity cycle in Proxima Centauri, we have to determine whether any flare occurred during our observations, since flare activity can mask the variations of activity due to the cycle, and it has to be filtered out before the analysis. In Figs. 3 and 4 we show the line profiles of the Ca II H and K and $H\alpha$ lines. Visual inspection of the temporal series of observations reveals the possible occurrence of several flares. The first one corresponds to the four observations 0300a to 0300d: the apparent flare goes from maximum to minimum, with the two central observations with similar levels of activity. Also, in the spectrum 0802b, all the lines are much stronger than in the previous one 0802a. Similar variations can be appreciated between observations 0303a and 0303b, 0305b and 0305a, and 0206a and 0206b, although in these cases the lines are not so intense. Using these considerations, we separated the flaring spectra from the “normal” ones. We excluded these flaring spectra – which are indicated in Table 1 with a ‘ \star ’ – from the rest of the analysis.

4. Behavior of $H\alpha$ with time

For the non-flaring spectra, we calculated a nightly average of the A index, shown in Table 2, which we examine in this section to determine the possible presence of an activity cycle. Using this data, we first calculated the Lomb-Scargle periodogram (Scargle 1982; Horne & Baliunas 1986) using the algorithm in-

Table 2. Nightly averaged A index. Column 1: the label used in Fig. 7; Col. 2: the xJD at the beginning of the observations; Col. 3: the quantity of spectra averaged; Col. 4: the total exposure time (in minutes); Col. 5: the average index.

Label	xJD	N	t	A
0399	241.85	2	50	2.89
0300	627.82	2	90	2.50
0301_1	972.78	2	120	2.14
0301_2	974.70	2	180	2.00
0701	1096.46	2	180	2.84
0302	1364.69	1	45	2.16
0602	1451.66	2	90	2.13
0802	1519.50	1	45	2.84
0303_1	1715.75	1	45	2.28
0303_2	1716.60	7	420	2.63
0903	1895.51	2	66	2.46
0604_1	2160.59	2	90	2.35
0604_2	2161.51	5	300	2.00
0904	2274.48	2	60	2.48
0305	2448.78	1	45	2.61
0605_1	2523.55	6	360	2.46
0605_2	2543.60	2	180	2.54
0805	2600.51	2	160	2.66
0206	2780.86	1	80	2.42

cluded in Press et al. (1992). This periodogram is a method to estimate the power spectrum (in the frequency domain), when observation times are unevenly spaced, and normalizes the spectrum in such a way that it is possible to measure the significance of the peaks. The amplitude of the periodogram at each frequency point is identical to the equation that would be obtained estimating the harmonic content of a data set, at a given frequency, by linear least-squares fitting to an harmonic function of time (Press et al. 1992). We show this periodogram in Fig. 5.

It can be seen in the figure that there is a distinct peak at 442 days, with a significance of 65%. In other words, a period of 442 days is detected, with a *False Alarm Probability* (FAP) of 35%. It is worth noting that this FAP is very good, since the activity cycles are neither harmonic nor exactly periodic. Other less significant peaks are present, the most important one corresponding to 166 days with a FAP of 80%. This peak could correspond to a subharmonic of a year, which can appear due to the fact that our observations are carried out with a periodicity of approximately one year.

We also applied several techniques in the time domain to check the existence of this period. Basically, all of them start with the construction of the light curve (that is, the observed data as a function of phase for different trial periods). Then, this light curve is partitioned in several bins, whose quantity depends on the amount of data available. In the three cases, we chose a partition of two bins, due to the small number of data points.

The first of these techniques is the one outlined in Jurkevich (1971), which assumes that the real period is the one that minimize the dispersion, measured from the average, of the combined bins of the light curve. The second one (Marraco & Muzzio 1980) is an improvement of the first, which consists in measuring the dispersion relative to the least-squares straight line for each bin. Finally, Cincotta et al. (1995) instead of minimizing the dispersion, calculated the so-called Shannon entropy, which is a measure of the order of the data. Again, the real period will minimize this quantity.

In Fig. 6 we show the dispersion of the light curve – or the Shannon entropy – as a function of the trial period for each method. In all of them we find periods compatible within 10% with the one of ~ 442 days (420, 492, and 412 days). Also present are possible harmonics of a year (198, 359, and 1090 days). One should keep in mind that solar activity is not exactly periodic, since each cycle has a different length and intensity. Therefore, we believe that the agreement found between different methods is quite remarkable.

We also fit the data, by least-squares, with a harmonic function with a period of 442 days, and we obtained the curve shown in Fig. 7a. Also the fit is remarkably good here, again considering that the cycle is not exactly harmonic. Finally, in Fig. 7b we draw the associated light curve.

As measured from minimum to maximum, the amplitude of the period is around 25% in A . If we translate this amplitude to the S index, using the slope of Fig. 2, we find a variation of about 130% in a cycle, to be compared with a solar variation for S of only $\sim 30\%$ (Baliunas et al. 1995). This much larger variability is consistent with the fact that Proxima Centauri is an extremely active star. Since there are no systematic studies of activity variations for M stars so far (e.g., see Baliunas et al. 1995), we cannot compare with any other similar star.

Finally, we checked the accuracy of the result of Fig. 5 using the sunspot numbers taken from the National Geophysical Data Center. To do so, we took a sample of the solar data with the same phase intervals that we have in our data for Proxima, we added Gaussian noise with errors of 10% at each point, and we computed the Lomb-Scargle periodogram. We repeated this procedure 1000 times with random starting dates.

For each periodogram, we considered the period with maximum significance (or minimum FAP) as the detected period. In Fig. 8 we plot the histogram of these detected periods. The full line shows only the periods with $FAP \leq 0.35$. We see that the correct period (10 to 12 years) was detected in 62% of the periodograms and in 44% of the cases with a $FAP \leq 0.35$. Only in 6% of the cases was a “false” period detected with a $FAP \leq 0.35$.

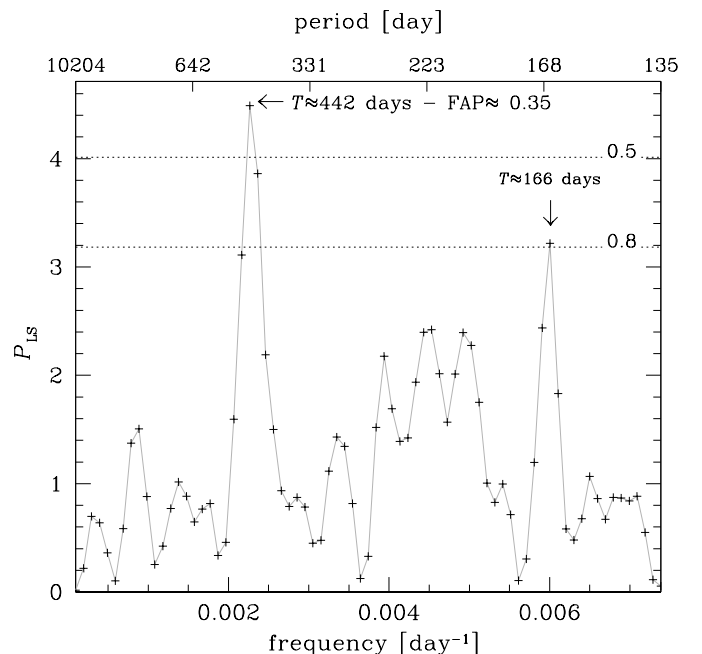


Fig. 5. Lomb-Scargle periodogram of the data of Table 2. The False Alarm Probability levels of 50 and 80% are shown.

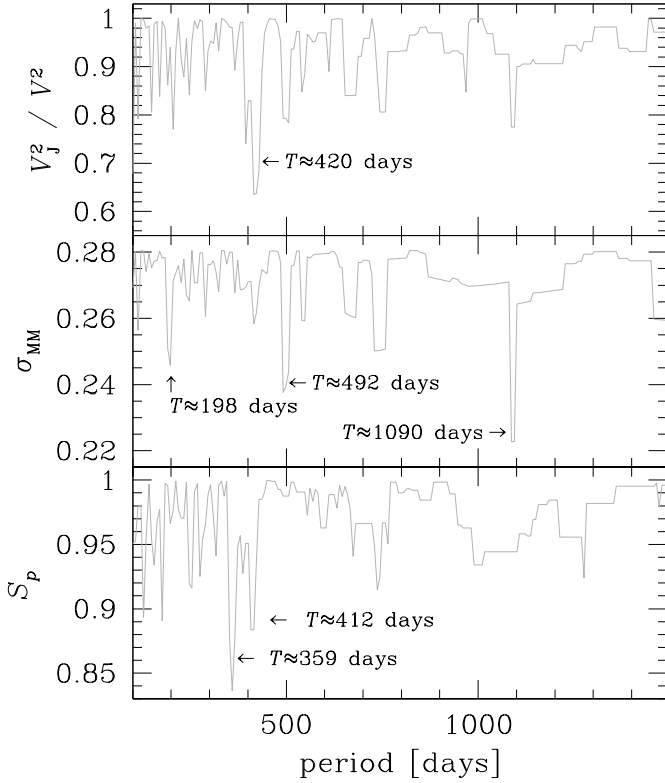


Fig. 6. The results of the three different methods employed that involve light-curve dispersion measurements: in the higher panel, the relative Jurkevich (1971) dispersion; in the middle panel, the Marraco & Muzzio (1980) dispersion; and in the lower panel, the Shannon entropy (Cincotta et al. 1995), for the data of Table 2.

Therefore, if this star has a cyclic behavior similar to the solar one, the probability of detecting it in our observations is $P \sim 60\%$ and the probability of detecting it with a $\text{FAP} \leq 0.35$

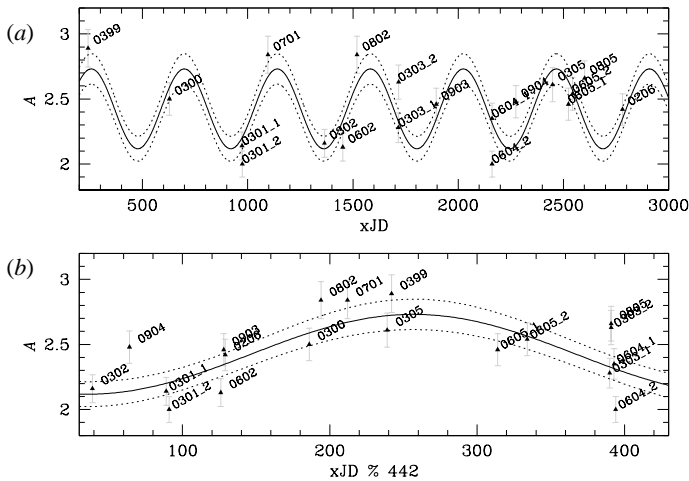


Fig. 7. *a)* A index vs. time, assuming errors of 5% for each point. The full curve is the least-squares fit to the data of Table 2 after establishing a harmonic function of period 442 days. The dotted curves represent the $\pm 2\sigma$ deviations. *b)* Light curve of the same data.

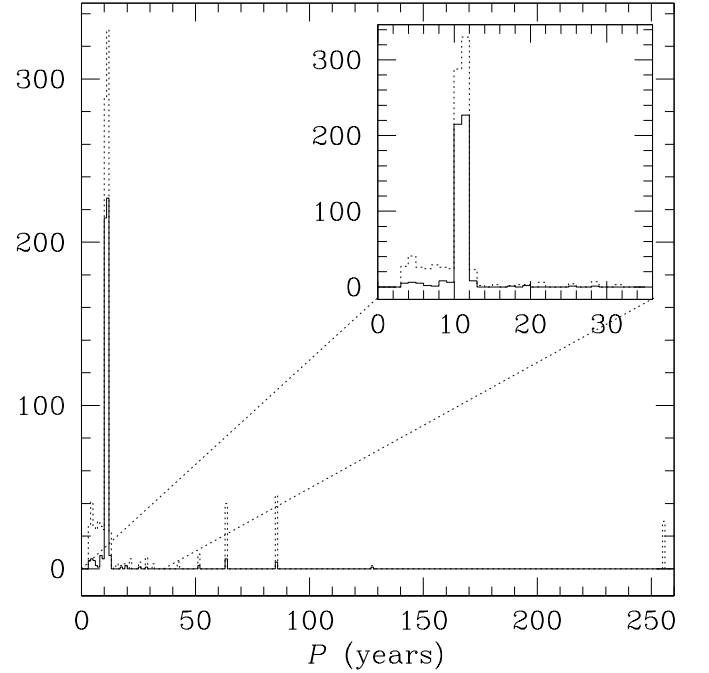


Fig. 8. Histogram of the detected periods (the periods for which we found the maxima P_{LS}) for a sample of 1000 different sets taken from the Sun. The full line shows only the periods with $\text{FAP} \leq 0.35$ and the dotted line shows all the cases.

is $P \sim 45\%$. On the other hand, if a period is detected with a $\text{FAP} \leq 0.35$, its value is correct with a probability of $P \sim 90\%$.

5. Discussion

In this paper we found strong evidence of a cyclic activity in the dMe star Proxima Centauri, with a period of $\sim 442 \text{ days} \pm 10\%$. Similar values for the period were found from the Lomb-Scargle periodogram and using three different techniques in the time domain. We were also able to determine that the activity variations outside of flares amount to 130% in S , four times larger than for the Sun.

As we mentioned before, the possible existence of an activity cycle in this star is mentioned in three previous papers. First, Haisch et al. (1990) found some evidence *suggesting* a stellar cycle, although they did not estimate its period. Guinan & Morgan (1996) found some manifestation that in 1995 Proxima was near a minimum of activity, again without an estimate of its period. In a more detailed study, Benedict et al. (1998a) found some hints of an activity cycle of about 1100 days, compatible with the minimum activity around 1995, although they had some gaps in temporal coverage. The middle point of what they consider minimum activity corresponds to JD 2 449 750. If we extrapolate our period back in time, taking into account that in JD 2 451 500 we have minimum activity, we find that in JD 2 449 732 we also have minimum activity, very close to what Benedict et al. (1998a) found. However, the data used in these two last works were also used to study the rotational period of this star, giving very different results: Guinan & Morgan (1996) found $P_{\text{rot}} = 31.5 \pm 1.5$ days and Benedict et al. (1998a) determined $P_{\text{rot}} = 83.5$ days. On the other hand, Kürster et al. (1999) did not find any evidence for the rotation periods found in these two works, based on very precise radial velocities of Proxima Centauri, which they analyze using both the Scargle periodogram and a sine-fitting routine, which

minimize χ^2 taking into account data errors. Therefore, we believe that our value of ~ 442 days for the cycle is more reliable, in particular because all the methods we employed give similar values for the period, and because we estimated, using solar data, that if a cycle is present, the period we found is the correct one with a probability $P \sim 90\%$.

Concerning the flare frequency, Walker (1981) predicts a flare of intensity greater than $5 \cdot 10^{27}$ in the U band once every 0.8 hr. For the most intense flares, the predicted frequency falls to one every 31 hr. In our case, we observed Proxima for ~ 54 hr, detecting two very strong flares (0300a to d and 0802b) and three weaker ones (0303a, 0305b, and 0206a) in this period. Therefore, we found a frequency of one flare every 10 hr.

It is generally accepted that magnetic activity results from the generation of a large-scale toroidal field by the action of differential rotation on a poloidal field, at the interface between the convective envelope and the radiative core (Parker 1975; Spiegel & Zahn 1992). This is the $\alpha\Omega$ dynamo, which predicts a strong correlation between activity and rotation, which is in fact observed for stars from F to early M. This theory also explains the fact that young rapid rotators – which have larger differential rotation – have higher activity levels than old slower rotators, with less differential rotation and therefore a less important dynamo effect.

On the other hand, stars ranging from M3 to M9 are thought to be fully convective, and therefore they do not support an $\alpha\Omega$ dynamo. It has been argued (Barnes 2003) that fully convective stars do not possess large-scale dynamos, and that their rotational morphology are dominated instead by small-scale turbulent fields. Nevertheless, there is plenty of observational evidence that slow late-type rotators like dMe stars have strong magnetic fields, with filling factors larger than for earlier stars and enhanced activity (Mochnacki & Zirin 1980; Hawley 1989; Mauas & Falchi 1996).

Recently, Chabrier & Küker (2006) showed that these cool objects can support large-scale magnetic fields by a pure α^2 dynamo process. In this dynamo, helicity is generated by the action of the Coriolis force on the convective motions in a rotating, stratified fluid, and produces an amplification of the mean magnetic field. Moreover, these fields can produce high levels of activity like the ones observed in M stars. This α^2 dynamo does not predict a cyclic activity. However, our observations suggest that this cool star does have a clear period.

The activity cycles measured in earlier stars (F to K) are all longer than 2.5 years (Baliunas et al. 1995), to be compared to the one we found for Proxima Centauri, of only 1.2 years. On the other hand, the variation of the activity levels is much larger for this star than for earlier-type ones. As we explained, the dynamo models show that the generation of activity in M stars is a very different phenomenon than in earlier stars, i.e., stars with a radiative core and an outer convection zone. It is desirable to confirm the existence of a cycle in Prox Cen and its period, and to explore other M stars near the limit where stars become fully convective, to constrain the dynamo at work in these stars.

Acknowledgements. The CCD and data acquisition system at CASLEO has been partly financed by R. M. Rich through U.S. NSF grant AST-90-15827.

References

- Allen, C. W. 1976, *Astrophysical Quantities* (Astrophysical Quantities, London: Athlone (3rd edition), 1976)
- Baliunas, S. L., Donahue, R. A., Soon, W., & Henry, G. W. 1998, in ASP Conf. Ser. 154: Cool Stars, Stellar Systems, and the Sun, 153–+
- Baliunas, S. L., Donahue, R. A., Soon, W. H., et al. 1995, *ApJ*, 438, 269
- Baliunas, S. L., Home, J. H., Porter, A., et al. 1985, *ApJ*, 294, 310
- Barnes, S. A. 2003, *ApJ*, 586, 464
- Benedict, G. F., McArthur, B., Nelan, E., et al. 1998a, *AJ*, 116, 429
- Benedict, G. F., McArthur, B., Nelan, E., et al. 1998b, in *Astronomical Society of the Pacific Conference Series*, 1212–+
- Byrne, P. B. & McKay, D. 1989, *A&A*, 223, 241
- Chabrier, G. & Küker, M. 2006, *A&A*, 446, 1027
- Cincotta, P. M., Mendez, M., & Nuñez, J. A. 1995, *ApJ*, 449, 231
- Cincunegui, C. & Mauas, P. J. D. 2002, in *ESA SP-477: Solspa 2001, Proceedings of the Second Solar Cycle and Space Weather Euroconference*, 91–94
- Cincunegui, C. & Mauas, P. J. D. 2004, *A&A*, 414, 699
- Demarque, P., Guenther, D. B., & van Altena, W. F. 1986, *ApJ*, 300, 773
- Doyle, J. G. 1987, *MNRAS*, 224, 1P
- Güdel, M., Audard, M., Reale, F., Skinner, S. L., & Linsky, J. L. 2004, *A&A*, 416, 713
- Güdel, M., Audard, M., Skinner, S. L., & Horvath, M. I. 2002, *ApJ*, 580, L73
- Guinan, E. F. & Morgan, N. D. 1996, *Bulletin of the American Astronomical Society*, 28, 942
- Haisch, B. M., Butler, C. J., Foing, B., Rodono, M., & Giampapa, M. S. 1990, *A&A*, 232, 387
- Haisch, B. M. & Linsky, J. L. 1980, *ApJ*, 236, L33
- Haisch, B. M., Linsky, J. L., Lampton, M., et al. 1977, *ApJ*, 213, L119
- Hawley, S. L. 1989, Ph.D. Thesis
- Henry, T. J., Soderblom, D. R., Donahue, R. A., & Baliunas, S. L. 1996, *AJ*, 111, 439
- Home, J. H. & Baliunas, S. L. 1986, *ApJ*, 302, 757
- Jurkevich, I. 1971, *Ap&SS*, 13, 154
- Kürster, M., Hatzes, A. P., Cochran, W. D., et al. 1999, *A&A*, 344, L5
- Marraco, H. G. & Muzzio, J. C. 1980, *PASP*, 92, 700
- Mauas, P. J. D. & Falchi, A. 1996, *A&A*, 310, 245
- Mochnacki, S. W. & Zirin, H. 1980, *ApJ*, 239, L27
- Parker, E. N. 1975, *ApJ*, 198, 205
- Patten, B. M. 1994, *Informational Bulletin on Variable Stars*, 4048, 1
- Perryman, M. A. C., Lindegren, L., Kovalevsky, J., et al. 1997, *A&A*, 323, L49
- Pettersen, B. R. 1980, *A&A*, 82, 53
- Press, W. H., Teukolsky, S. A., Vetterling, W. T., & Flannery, B. P. 1992, *Numerical recipes in C. The art of scientific computing* (Cambridge: University Press, —c1992, 2nd ed.)
- Reale, F., Güdel, M., Peres, G., & Audard, M. 2004, *A&A*, 416, 733
- Reale, F., Peres, G., Serio, S., Rosner, R., & Schmitt, J. H. M. M. 1988, *ApJ*, 328, 256
- Scargle, J. D. 1982, *ApJ*, 263, 835
- Ségransan, D., Kervella, P., Forveille, T., & Queloz, D. 2003, *A&A*, 397, L5
- Slee, O. B., Willes, A. J., & Robinson, R. D. 2003, *Publications of the Astronomical Society of Australia*, 20, 257
- Spiegel, E. A. & Zahn, J.-P. 1992, *A&A*, 265, 106
- Vaughan, A. H., Preston, G. W., & Wilson, O. C. 1978, *PASP*, 90, 267
- Walker, A. R. 1981, *MNRAS*, 195, 1029

List of Objects

‘Proxima Centauri’ on page 1

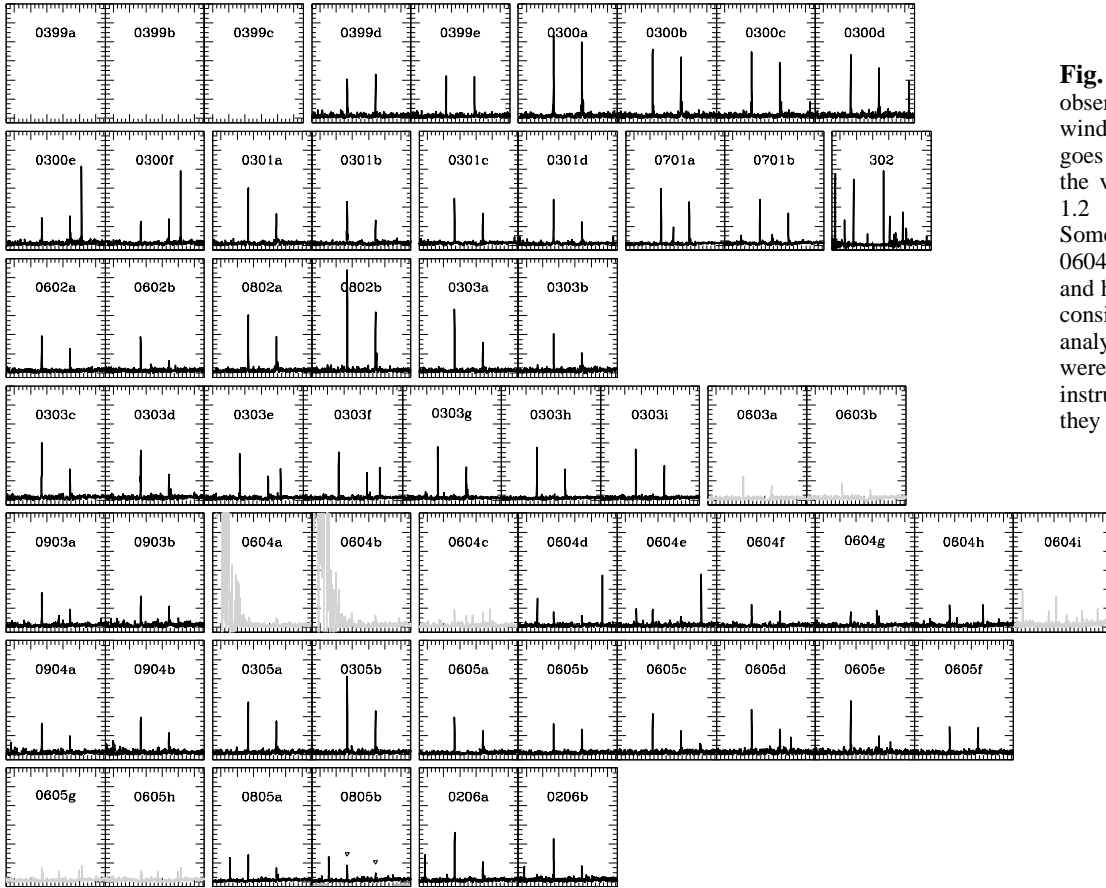


Fig. 3. Ca II region for each observation of Table 1. In each window the horizontal axis goes from 3890 to 4012 Å, and the vertical one from -0.05 to $1.2 \cdot 10^{-12} \text{ erg cm}^{-2} \text{ s}^{-1} \text{ Å}^{-1}$. Some spectra (0603a and b; 0604a, b, c, and i; and 0605g and h) are deficient and are not considered in the subsequent analysis. The first three spectra were acquired with a different instrumental configuration and they do not include this region.

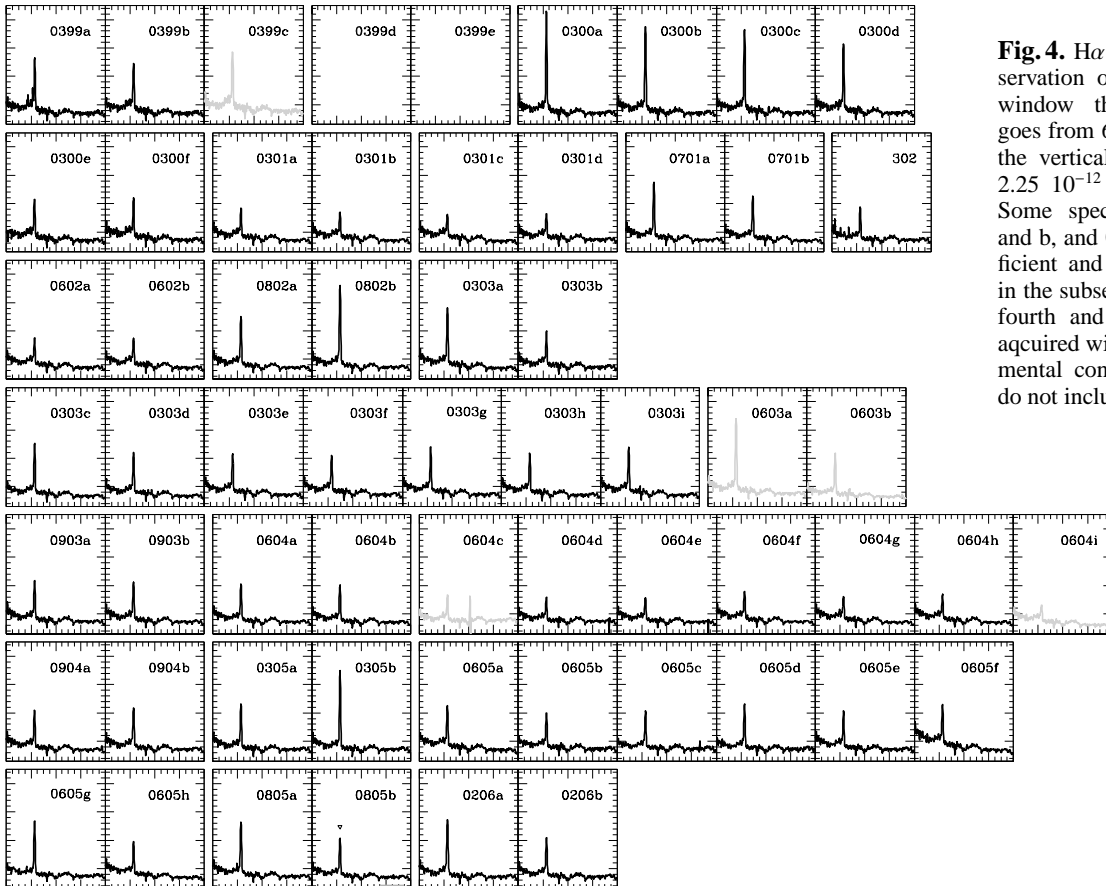


Fig. 4. $H\alpha$ region for each observation of Table 1. In each window the horizontal axis goes from 6540 to 6620 Å, and the vertical one from 0.15 to $2.25 \cdot 10^{-12} \text{ erg cm}^{-2} \text{ s}^{-1} \text{ Å}^{-1}$. Some spectra (0399c, 0603a and b, and 0604c and i) are deficient and are not considered in the subsequent analysis. The fourth and fifth spectra were acquired with a different instrumental configuration and they do not include this region.